

# Papain-capped gold nanoflowers: dual functionality as peroxidase mimic and 4-nitrophenol reduction catalysts

Dan Yan, Juan Liu, Yuanyuan Chen\*

Institute of Pharmaceutical Innovation, Hubei Province Key Laboratory of Occupational Hazard Identification and Control, School of Medicine, Wuhan University of Science and Technology, Wuhan, 430065, China

## ABSTRACT

A bifunctional ensemble of papain-capped gold nanoparticles (AuNFs) exhibits dual functionality, manifesting peroxidase-like and 4-nitrophenol reduction activities. The AuNFs, possessing an average size of approximately  $82.27 \pm 1.95$  nm, are synthesized under ambient conditions through the mediation of papain, wherein the reduction of  $\text{HAuCl}_4$  by ascorbic acid is facilitated. These nanoflowers are capable of catalyzing  $\text{H}_2\text{O}_2$  to oxidize the target 3,3,5,5-tetramethylbenzidine, resulting in the production of a visual color of blue. Therefore, a simple method providing a sensitivity of  $0.44 \mu\text{M}$  (signal/noise ratio = 2) and a linearity within the range of 0 to  $40 \mu\text{M}$  is available to detect  $\text{H}_2\text{O}_2$  by colorimetry. Subsequently, the chemical activity associated with the 4-NP (4-nitrophenol) reduction was studied, and it was found to exhibit a catalysis rate of  $0.29 \text{ min}^{-1}$ , surpassing that of alternative gold catalysts. These findings underscore the potential utility of our AuNFs in catalytic and biosensing applications.

**Keywords:** Gold nanoflower, peroxidase-like, 4-nitrophenol reduction, biomaterials, sensors

## 1. INTRODUCTION

4-Nitrophenol (4-NP) is integral to chemical manufacturing, serving as an organic intermediate in compounds like dyes, pharmaceuticals, and surfactants [1-6]. Despite its utility, 4-NP poses environmental hazards due to its toxicity to aquatic life and human health risks, primarily from industrial effluents [7-11]. The conversion of 4-nitrophenol to 4-aminophenol, an essential precursor used in manufacturing a wide range of critical organic chemicals, including analgesics and antipyretics, is challenging for reducing agents due to the inherent inertness of nitro groups [3, 5, 12, 13], particularly under ambient conditions. Therefore, there is an urgent need to identify a catalyst that is not only cost-effective, but also has exceptional efficiency and selective properties for facilitating 4-nitrophenol degradation [14-20].

Attributable to a substantial surface-to-volume ratio. Nanomaterials have garnered attention for their utilization as high-efficiency catalysts, with specific variants exhibiting peroxidase-like activities [21-30]. In particular, magnetic  $\text{Fe}_3\text{O}_4$  nanoparticles were found to have peroxidase-like activities, according to Yan's research [31]. Subsequently, two-dimensional materials like graphene oxide,  $\text{MoS}_2$ , and their composites similarly exhibit peroxidase-like activity [32-39]. In contrast, gold nanomaterials (AuNMs) are among the most pivotal enzymes, credited to their stability, biocompatibility, and unforeseen activities [40-46]. Among them, gold nanoflowers (AuNFs) have received extensive investigation due to their pronounced surface roughness and high-index facets [47, 48]. The catalytic process of AuNMs is typically assessed using a known response: the transformation with  $\text{NaBH}_4$  of 4-nitrophenol (4-NP) into a 4-aminophenol (4-AP) [49, 50]. Although different kinds of AuNMs have been widely reported as either enzyme mimics [51-53] or 4-NP reduction catalysts [54-57]. However, to our knowledge, there have been few reports of AuNFs exhibiting both peroxidase-like activity and reducing 4-nitrophenol (4-NP) activity.

In this piece of work, we have developed a green strategy to produce uniform AuNFs with both peroxidase-like and 4-nitrophenol (4-NP) reducing activity by template papain (Figure 1). Specifically, AuNFs provide a blue staining method for  $\text{H}_2\text{O}_2$  detection by facilitating the  $\text{H}_2\text{O}_2$ -based oxygenation of the enzyme candidate peroxidase inhibitor template

\* yychen@wust.edu.cn

3,3,5,5-tetramethylbenzidine (TMB). Furthermore, AuNFs activity for catalyzing degradation of 4-NP showed that AuNFs can also act as an efficient reduction catalyst.

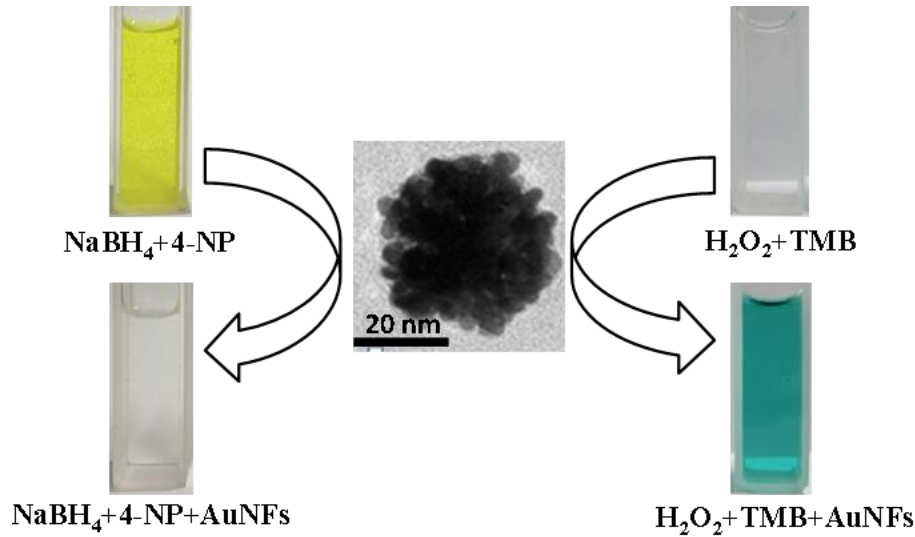


Figure 1. A bi-functional AuNFs catalyst with both peroxidase-like and 4-NP reduction activity has been synthesised by a green strategy with papain as the capping agent.

## 2. EXPERIMENTAL SECTION

### 2.1 Synthesis of AuNFs

AuNFs were synthesized following a previously established protocol with minor adaptations, as detailed in reference [58]. In a common method of synthesis, a liquid consisting of HAuCl<sub>4</sub> (0.2 mM) and papain (0.2 mg ml<sup>-1</sup>) was rapidly added to a predetermined amount of ascorbic acid (AA). After a brief period of gentle stirring for 2 minutes, the mixture was continuously agitated for the specified duration at ambient temperature, during which a rapid transition in coloration from a faint yellow hue to a deep blue shade was observed. Subsequently, the resulting gold samples underwent overnight dialysis to eliminate residual AA, HAuCl<sub>4</sub>, and other incidental byproducts.

### 2.2 Peroxidase-like activity of AuNFs

Catalytic studies were performed using 50 µg mL<sup>-1</sup> AuNFs in an amount of 600 µL of sodium acetate-acetic acid buffer at a 0.02 M concentration (pH 4, 25 °C). The substrate was either 600 µM TMB or 10 mM H<sub>2</sub>O<sub>2</sub>. Peroxidase-like activity was assessed by detection in situ at 652 nm in a Shimadzu UV2550 UV-vis spectrophotometer.

### 2.3 Detection of H<sub>2</sub>O<sub>2</sub>

H<sub>2</sub>O<sub>2</sub> was detected as follows: 300 µL H<sub>2</sub>O<sub>2</sub> at various concentrations was added to a mixture containing 180 µL TMB (2 mM) and 120 µL AuNFs stock concentration (50 µg mL<sup>-1</sup>). The resulting solution was utilized for time-course measurements conducted at a wavelength of 652 nm.

### 2.4 Catalysed reduction of 4-NPs

NaBH<sub>4</sub> solution (0.42 mol/L, 10 mL) was dissolved in 4-NP solution (0.175×10<sup>-3</sup> mol/L, 70 mL). For recording the UV-vis spectra at identical times, 100 µL of the AuNFs suspension (50 µg mL<sup>-1</sup>) was dissolved in 3 mL of 4-NP.

### 3. CONCLUSIONS AND DISCUSSION

#### 3.1 Characterisation of AuNFs

The as-prepared AuNFs displayed a blue suspension that remained stable for approximately one year (Figure 2a), attributed to the capping effect of papain. UV-vis spectra for the product showed a prominent maximum of 568 nm, indicative of the peak of the superficial plasmon resonance, which indicates that Au(0) starts to form. Crystal pattern analysis of the as-prepared Au(0) was carried out by XRD (Figure 2b), exhibiting close conformity with the fcc Au as documented in the PDF card (JCPDS file number 04-0784). SEM and TEM have been applied to characterize the morphological properties of the AuNFs. SEM imagery (Figure 2c-d) revealed the presence of abundant Au nanostructures in a flower-like configuration with a uniform size of  $82.27 \pm 1.95$  nm, further corroborated by TEM imagery (Figure 2e). The electron diffraction pattern corresponded to the fcc structure of gold (Figure 2e inset). The HRTEM image (Figure 2f) delineated that the nanoflowers comprised a significant quantity of AuNPs, exhibiting distinct interplanetary spacing of 0.238 nm (111). Optimization of the effect of AA, a reducing agent, on AuNFs synthesis yielded an optimal concentration of 0.85 mM (Figure S1). The protein and  $\text{AuCl}_4^-$  complex structures in solution would be influenced significantly by the pH of the system. Thus, the influence of pH on the production of AuNFs needs to be investigated and optimized at pH 6 (Figure S2).

#### 3.2 Intrinsic peroxidase-like activity of AuNFs and $\text{H}_2\text{O}_2$ detection

Since colorless TMB is oxidized in the presence of a catalysator to a colored product, the TMB- $\text{H}_2\text{O}_2$  reaction is the model reaction used to assess the peroxidase-like action by AuNFs (Figure S3). Figure 3a demonstrates that the absorption of the TMB oxidized product increases with time for the mixed TMB,  $\text{H}_2\text{O}_2$ , and AuNFs. Figure 3b shows that neither  $\text{H}_2\text{O}_2$  nor as-received AuNFs alone can efficiently oxidize TMB to generate the blue colour. Hence, the oxidization of TMB results is directly proportional to the decomposition of  $\text{H}_2\text{O}_2$  caused by the as-received AuNFs. Thus, TMB oxidation results from the decomposition of  $\text{H}_2\text{O}_2$  by the AuNFs as they are obtained. Notably, bare papain exhibits slight peroxidase-like activity, potentially attributable to the presence of multiple His residues, which stabilize radicals capable of effectively oxidizing TMB to produce colored oxTMB [59, 60]. Figure 3c shows an improvement in the velocity at which the reaction takes place as the AuNF concentration is raised up to  $60 \mu\text{g mL}^{-1}$ . The pH value was optimized to be 4 (Figure 3d).  $\text{H}_2\text{O}_2$  is capable of adsorbing onto the surface of AuNFs, in which the  $\text{H}_2\text{O}_2$  O-O bond is able to cleave to produce  $\text{HO}^\bullet$  radicals. The resultant  $\text{HO}^\bullet$  radicals could potentially be stabilized by papain (zeta potential: +14.9 mV) *via* partial electron exchange interactions, thereby augmenting the catalytic prowess of positively charged AuNFs [61].

The accelerated oxidation of  $\text{H}_2\text{O}_2$  by AuNFs shows evidence of concentration-dependent catalysis, making the system potentially applicable for  $\text{H}_2\text{O}_2$  detection. The relationship between the concentration of  $\text{H}_2\text{O}_2$  and TMB absorbance is illustrated in Figure 3e. A linear correlation with a correlation coefficient of 0.9989 is found for the 0-40  $\mu\text{M}$  span (Figure 3f). The resulting regression equation is given as  $\text{Absorbance} = 0.009C + 0.004$  (where C is the  $\text{H}_2\text{O}_2$  concentration in  $\mu\text{M}$ ), giving a limit of quantitation of 0.44  $\mu\text{M}$  (S/N = 2). This detection limit notably surpasses those observed in other gold-based sensors [52, 62].

#### 3.3 Application for 4-NP reduction

The reducibility from 4-NP to 4-AP towards  $\text{NaBH}_4$  has been used to investigate the reductive catalytic performance of the prepared AgNFs. As observed from the UV-visible spectral data (Figure 4a), the development from 4-AP with the addition of AuNFs was followed by the occurrence at 300 nm of a peak associated with a drop in the intensity of the 400 nm peak. The relationship between  $\ln(C_t/C_0)$  and time (min) showed linearity ( $\ln(C_t/C_0) = -0.2915t + 0.1896$ ,  $R^2 = 0.984$ ), where  $C_0$  and  $C_t$  are 4-NP levels at instant 0 and instant t, individually (Figure 4b). The ratio of absorbance,  $A_t/A_0$ , could be replaced by the concentration ratio,  $C_t/C_0$  (i.e.  $C_t/C_0 = A_t/A_0$ ), since the 4-NP concentration is proportionate to the absorbance. The catalytic efficiency ( $0.29 \text{ min}^{-1}$ ) is higher than other gold catalysts [57, 63].

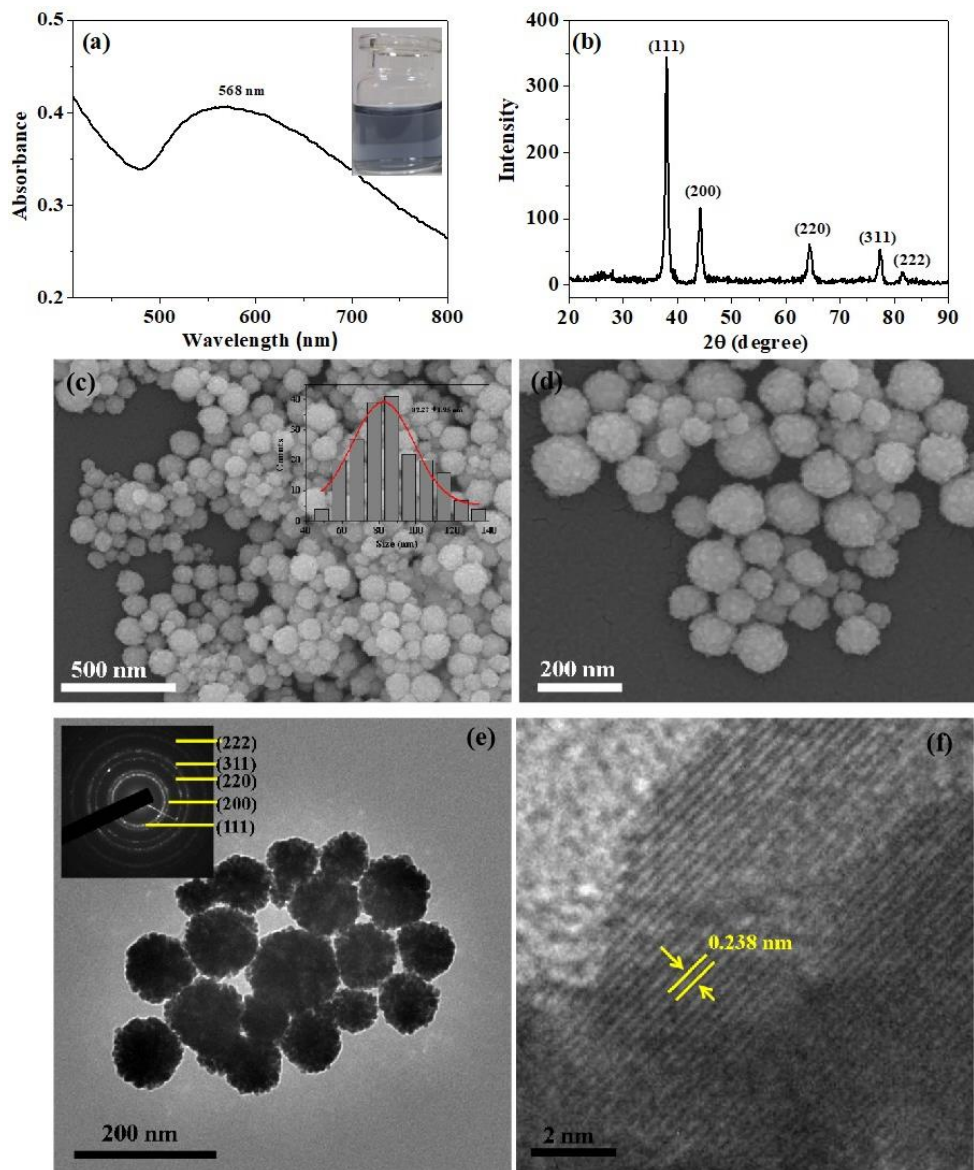


Figure 2. Characterization of AuNFs. (a) UV-vis spectra and optical photo of as-prepared AuNFs (inset). (b) XRD pattern. (c) SEM image and corresponding size distributions of AuNFs (inset). (d) magnified SEM image. (e) TEM image and associated SAED sample (inset). (f) HR-TEM image.

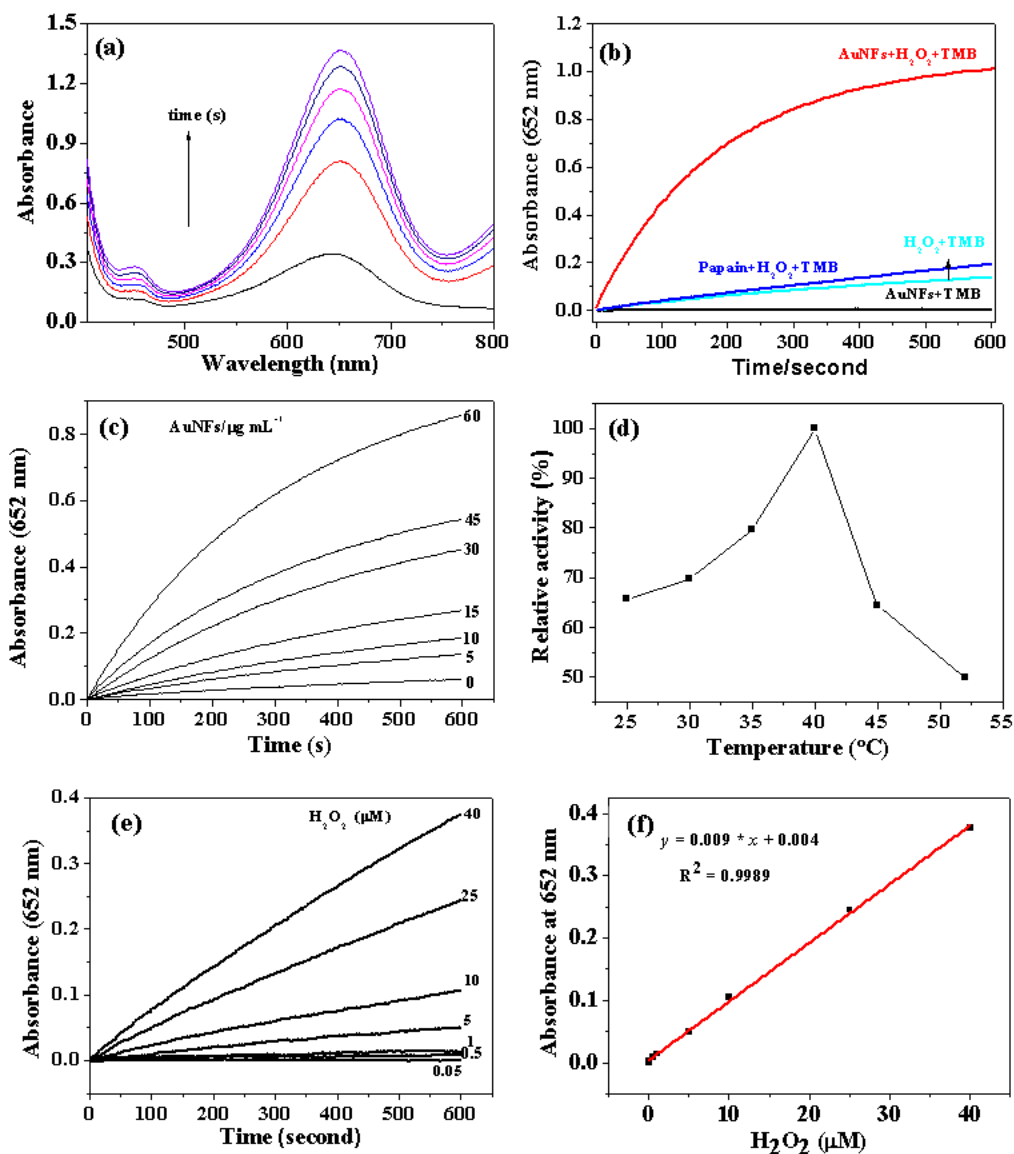


Figure 3. AuNF peroxidase-like activity. (a) UV-vis spectrum of the solution of a mixture of TMB and H<sub>2</sub>O<sub>2</sub>, taken at the same intervals after adding 50 µg mL<sup>-1</sup> of AuNFs in a pH 4 system. (b) Time dependency of changes in absorbance at 652 nm of TMB solutions in the presence of AuNFs, papain, H<sub>2</sub>O<sub>2</sub>, AuNFs, and H<sub>2</sub>O<sub>2</sub>, individually. (c) Changes in the absorbance at 652 nm for the TMB and the H<sub>2</sub>O<sub>2</sub> system in the presence of AuNFs at different concentrations. (d) Peroxidase-like activity of AuNFs as a function of pH. (e) Changes in absorbance at 652 nm for various H<sub>2</sub>O<sub>2</sub> concentrations. (f) Calculate from (e) the linearity of the calibration curve for H<sub>2</sub>O<sub>2</sub>.

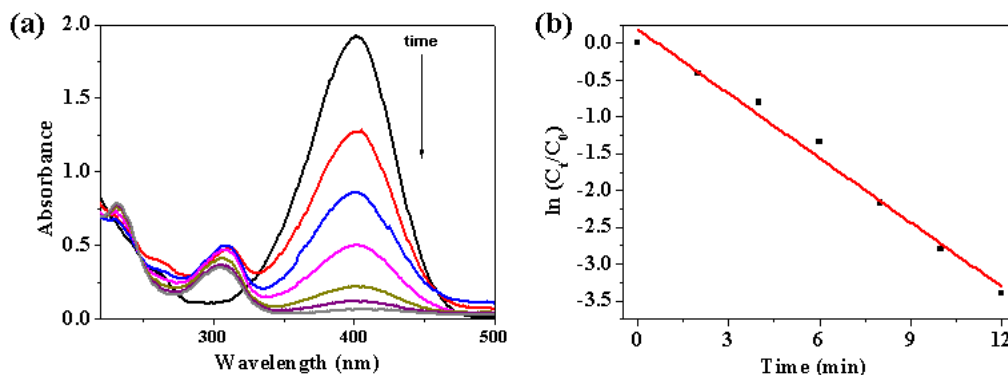


Figure 4. 4-NP reduction. UV-vis spectrums of 4-NP as reduced with NaBH<sub>4</sub> in the presence of AuNFs ranging in time from 0 to 300 s. b) Plotting ln(C<sub>t</sub>/C<sub>0</sub>) as a function of time taken from part (a).

#### 4. CONCLUSION

We established that papain-capped AuNFs prepared by a green strategy show both peroxidase-like and 4-NP reduction activity. The colorimetric method has a robust sensitivity to hydroperoxide (H<sub>2</sub>O<sub>2</sub>), with a detectability level of 0.44 μM and high sensitivity. Moreover, the catalytic capability of AuNFs in the decrease of 4-NP is remarkably efficient, evidenced by catalytic activity of 0.29 min<sup>-1</sup>. Our work expands the utilization of biomolecule-capped AuNFs in catalysis and biosensing applications.

#### ACKNOWLEDGEMENTS

This work was funded by the PhD Research Foundation of Wuhan University of Science and Technology (1170040).

#### REFERENCES

- [1] Ali, F., Khan, S. B., Shaheen, N. and Zhu, Y. Z., "Eggshell membranes coated chitosan decorated with metal nanoparticles for the catalytic reduction of organic contaminates," *Carbohydr. Polym.* 259, 117681 (2021).
- [2] Mejía, Y. R. and Bogireddy, N. K. R., "Reduction of 4-nitrophenol using green-fabricated metal nanoparticles," *RSC Adv.* 12(29), 18661-18675 (2022).
- [3] Neal, R. D., Inoue, Y., Hughes, R. A. and Neretina, S., "Catalytic reduction of 4-nitrophenol by gold catalysts: the influence of borohydride concentration on the induction time," *J. Phys. Chem. C.* 123(20), 12894-12901 (2019).
- [4] Abd Razak, N. F. and Shamsuddin, M., "Catalytic reduction of 4-nitrophenol over biostabilized gold nanoparticles supported onto thioctic acid functionalized silica-coated magnetite nanoparticles and optimization using response surface methodology," *Inorg. Nano-Met Chem.* 50(7), 489-500 (2020).
- [5] Bogireddy, N. K. R., Sahare, P., Pal, U., Méndez, S. F. O., Gomez, L. M. and Agarwal, V., "Platinum nanoparticle-assembled porous biogenic silica 3D hybrid structures with outstanding 4-nitrophenol degradation performance," *Chem. Eng. J.* 388(15), 124237 (2020).
- [6] Shen, W., Qu, Y., Pei, X., Li, S., You, S., Wang, J., Zhang, Z. and Zhou, J., "Catalytic reduction of 4-nitrophenol using gold nanoparticles biosynthesized by cell-free extracts of *Aspergillus* sp. WL-Au," *J. Hazard. Mater.* 321(20), 299-306 (2017).
- [7] Xiong, Z., Zhang, H., Zhang, W., Lai, B. and Yao, G., "Removal of nitrophenols and their derivatives by chemical redox: a review," *Chem. Eng. J.* 359(20), 13-31 (2019).
- [8] Zhao, P., Feng, X., Huang, D., Yang, G. and Astruc, D., "Basic concepts and recent advances in nitrophenol reduction by gold-and other transition metal nanoparticles," *Coord. Chem. Rev.* 287(19), 114-136 (2015).
- [9] Dong, X.-Y., Gao, Z.-W., Yang, K.-F., Zhang, W.-Q. and Xu, L.-W., "Nanosilver as a new generation of silver catalysts in organic transformations for efficient synthesis of fine chemicals," *Catal. Sci. Technol.* 5(5), 2554-2574 (2015).
- [10] Qin, L., Huang, D., Xu, P., Zeng, G., Lai, C., Fu, Y., Yi, H., Li, B., Zhang, C. and Cheng, M. J. J. O. C., "In-situ deposition of gold nanoparticles onto polydopamine-decorated g-C<sub>3</sub>N<sub>4</sub> for highly efficient reduction of nitroaromatics in environmental water purification," *J. Colloid. Interf. Sci.* 534(24), 357-369 (2019).

- [11] Dong, J., Yang, P., Chen, J., Ji, Y. and Lu, J., "Nitrophenolic byproducts formation during sulfate radical oxidation and their fate in simulated drinking water treatment processes," *Water Res.* 224(4), 119054 (2022).
- [12] Bogireddy, N. K. R., Mejia, Y. R., Aminabhavi, T. M., Barba, V., Becerra, R. H., Flores, A. D. A. and Agarwal, V., "The identification of byproducts from the catalytic reduction reaction of 4-nitrophenol to 4-aminophenol: A systematic spectroscopic study," *J. Environ. Manage.* 316(9), 115292 (2022).
- [13] Abd Razak, N. F. and Shamsuddin, M., "Catalytic reduction of 4-nitrophenol over biostabilized gold nanoparticles supported onto thioctic acid functionalized silica-coated magnetite nanoparticles and optimization using response surface methodology," *Inorganic Nano-Metal Chemistry* 50(7), 489-500 (2020).
- [14] Chakraborty, U., Bhanjana, G., Kaur, N., Sharma, R., Kaur, G., Kaushik, A. and Chaudhary, G. R., "Microwave-assisted assembly of Ag<sub>2</sub>O-ZnO composite nanocones for electrochemical detection of 4-Nitrophenol and assessment of their photocatalytic activity towards degradation of 4-Nitrophenol and Methylene blue dye," *J. Hazard. Mater.* 416(5), 125771 (2021).
- [15] Din, M. I., Khalid, R., Hussain, Z., Hussain, T., Mujahid, A., Najeeb, J. and Izhar, F., "Nanocatalytic assemblies for catalytic reduction of nitrophenols: a critical review," *Crit. Rev. Anal. Chem.* 50(4), 322-338 (2020).
- [16] Zhang, J., Geng, W., Shi, L., Yang, C., Zhang, X., Geng, Y., Hirani, R. a. K., Xu, X., Wei, J. and Jing, Y., "One-pot synthesis of boron and nitrogen co-doped nanocarbons for efficient catalytic reduction of nitrophenols," *Chem. Eng. J.* 439(12), 135733 (2022).
- [17] Zhang, N., Wu, Y., Yuen, G. and De Lannoy, C.-F., "Ultrafiltration Pd-immobilized catalytic membrane microreactors continuously reduce nitrophenol: A study of catalytic activity and simultaneous separation," *Sep. Purif. Technol.* 312(16), 123318 (2023).
- [18] Zheng, A. L. T., Teo, E. Y. L., Seenivasagam, S., Yiu, P. H., Boonyuen, S., Chung, E. L. T., Lease, J. and Andou, Y., "Nanostructures embedded on porous materials for the catalytic reduction of nitrophenols: a concise review," *J. Porous Mater.* (2), 1-19 (2024).
- [19] Asif, I., Baig, N., Sher, M., Ul-Hamid, A., Altaf, M., Mumtaz, A. and Sohail, M., "MOF derived novel zero-valent iron@ graphitic carbon-based nanoreactors for selective reduction of hazardous 4-nitrophenol," *Clean.Eng.Technol* 2(4), 100081 (2021).
- [20] Ismail, M., Khan, M., Khan, M. A., Akhtar, K., Asiri, A. M. and Khan, S. B., "Plant-supported silver nanoparticles: Efficient, economically viable and easily recoverable catalyst for the reduction of organic pollutants," *Appl. Organomet. Chem.* 33(8), e4971 (2019).
- [21] Dhiman, N., Ghosh, S., Mishra, Y. K. and Tripathi, K. M., "Prospects of nano-carbons as emerging catalysts for enzyme-mimetic applications," *Mat. Adv.* 3(7), 3101-3122 (2022).
- [22] Villalba-Rodríguez, A. M., Martínez-Zamudio, L. Y., Martínez, S. a. H., Rodríguez-Hernández, J. A., Melchor-Martínez, E. M., Flores-Contreras, E. A., González-González, R. B. and Parra-Saldívar, R., "Nanomaterial constructs for catalytic applications in biomedicine: nanobiocatalysts and nanozymes," *Top. Catal.* 66(9), 707-722 (2023).
- [23] Stasyuk, N., Smutok, O., Demkiv, O., Prokopiv, T., Gayda, G., Nisnevitch, M. and Gonchar, M., "Synthesis, catalytic properties and application in biosensorics of nanozymes and electronanocatalysts: A review," *Sensors* 20(16), 4509 (2020).
- [24] Mahmoudpour, M., Ding, S., Lyu, Z., Ebrahimi, G., Du, D., Dolatabadi, J. E. N., Torbati, M. and Lin, Y., "Aptamer functionalized nanomaterials for biomedical applications: Recent advances and new horizons," *Nano Today* 39(3), 101177 (2021).
- [25] Tan, L. L., Wei, M., Shang, L. and Yang, Y. W., "Cucurbiturils-mediated noble metal nanoparticles for applications in sensing, sers, theranostics, and catalysis," *Adv. Funct. Mater.* 31(1), 2007277 (2021).
- [26] Wang, X., Zhong, X., Li, J., Liu, Z. and Cheng, L., "Inorganic nanomaterials with rapid clearance for biomedical applications," *Chem. Soc. Rev.* 50(15), 8669-8742 (2021).
- [27] Pedone, D., Moglianetti, M., De Luca, E., Bardi, G. and Pompa, P. P., "Platinum nanoparticles in nanobiomedicine," *Chem. Soc. Rev.* 46(16), 4951-4975 (2017).
- [28] Liu, L., Hao, Y., Deng, D. and Xia, N., "Nanomaterials-based colorimetric immunoassays," *Nanomater* 9(3), 316 (2019).
- [29] Ahmadi, S., Rahimizadeh, K., Shafiee, A., Rabiee, N. and Iravani, S., "Nanozymes and their emerging applications in biomedicine," *Process Biochem.* 131(5), 154-174 (2023).
- [30] Huang, Y., Ren, J. and Qu, X., "Nanozymes: classification, catalytic mechanisms, activity regulation, and applications," *Chem. Rev.* 119(6), 4357-4412 (2019).

- [31] Gao, L., Zhuang, J., Nie, L., Zhang, J., Zhang, Y., Gu, N., Wang, T., Feng, J., Yang, D. and Perrett, S., "Intrinsic peroxidase-like activity of ferromagnetic nanoparticles," *Nat. Nanotechnol.* 2(9), 577-583 (2007).
- [32] Ali, S. R. and De, M., "Thiolated ligand-functionalized MoS<sub>2</sub> nanosheets for peroxidase-like activities," *ACS Applied Nano Materials* 4(11), 12682-12689 (2021).
- [33] Muráth, S., Alsharif, N. B., Sáringér, S., Katana, B., Somosi, Z. and Szilagyi, I., "Antioxidant materials based on 2D nanostructures: A review on recent progresses," *Crystals* 10(3), 148 (2020).
- [34] Liu, J., Du, J., Su, Y. and Zhao, H., "A facile solvothermal synthesis of 3D magnetic MoS<sub>2</sub>/Fe<sub>3</sub>O<sub>4</sub> nanocomposites with enhanced peroxidase-mimicking activity and colorimetric detection of perfluorooctane sulfonate," *Microchem. J.* 149(11), 104019 (2019).
- [35] Mei, L., Zhu, S., Yin, W., Chen, C., Nie, G., Gu, Z. and Zhao, Y., "Two-dimensional nanomaterials beyond graphene for antibacterial applications: current progress and future perspectives," *Theranostics* 10(2), 757 (2020).
- [36] Ping, J., Fan, Z., Sindoro, M., Ying, Y. and Zhang, H., "Recent advances in sensing applications of two-dimensional transition metal dichalcogenide nanosheets and their composites," *Adv. Funct. Mater.* 27(19), 1605817 (2017).
- [37] Yin, W., Yu, J., Lv, F., Yan, L., Zheng, L. R., Gu, Z. and Zhao, Y., "Functionalized nano-MoS<sub>2</sub> with peroxidase catalytic and near-infrared photothermal activities for safe and synergetic wound antibacterial applications," *ACS Nano* 10(12), 11000-11011 (2016).
- [38] Rohaizad, N., Mayorga-Martinez, C. C., Fojtů, M., Latiff, N. M. and Pumera, M., "Two-dimensional materials in biomedical, biosensing and sensing applications," *Chem. Soc. Rev.* 50(1), 619-657 (2021).
- [39] Peng, J. and Weng, J., "Enhanced peroxidase-like activity of MoS<sub>2</sub>/graphene oxide hybrid with light irradiation for glucose detection," *Biosens. Bioelectron.* 89(10), 652-658 (2017).
- [40] Peng, L., Li, B. L., Zhou, C. W., Li, N. B., Setyawati, M. I. and Zou, H. L., "'Naked-eye' recognition: Emerging gold nano-family for visual sensing," *Appl. Mater. Today* 11(3), 166-188 (2018).
- [41] Mohamad, A., Rizwan, M., Keasberry, N. A., Nguyen, A. S., Dai Lam, T. and Ahmed, M. U., "Gold-microrods/Pd-nanoparticles/polyaniline-nanocomposite-interface as a peroxidase-mimic for sensitive detection of tropomyosin," *Biosens. Bioelectron.* 155(16), 112108 (2020).
- [42] Dí az, S. A., Choo, P., Oh, E., Susumu, K., Klein, W. P., Walper, S. A., Hastman, D. A., Odom, T. W. and Medintz, I. L., "Gold nanoparticle templating increases the catalytic rate of an amylase, maltase, and glucokinase multienzyme cascade through substrate channeling independent of surface curvature," *ACS Catalysis* 11(2), 627-638 (2020).
- [43] Zhu, D., Zhang, X., Han, Y., Luan, X. and Wei, G., "Biomimetic gold nanomaterials for biosensing, bioimaging and biotherapy: A mini-review," *Sens. Diagn.* 2(2), 320-336 (2023).
- [44] Wang, Z., Ye, M., Ma, D., Shen, J. and Fang, F., "Engineering of <sup>177</sup>Lu-labeled gold encapsulated into dendrimeric nanomaterials for the treatment of lung cancer," *Journal of Biomaterials Science, Polymer Edition* 33(2), 197-211 (2022).
- [45] Tessaro, L., Aquino, A., Panzenhagen, P., Joshi, N. and Conte-Junior, C. A., "A systematic review of the advancement on colorimetric nanobiosensors for SARS-CoV-2 detection," *J. Pharm. Biomed. Anal.* 222(15), 115087 (2023).
- [46] Lin, Y., Ren, J. and Qu, X., "Nano-gold as artificial enzymes: hidden talents," *Adv. Mater.* 26(25), 4200-4217 (2014).
- [47] Patel, A. S., Juneja, S., Kanaujia, P. K., Maurya, V., Prakash, G. V., Chakraborti, A. and Bhattacharya, J. J. N.-S., "Gold nanoflowers as efficient hosts for SERS based sensing and bio-imaging," *Nano-Structures & Nano-Objects* 16(1), 329-336 (2018).
- [48] Huang, P., Pandoli, O., Wang, X., Wang, Z., Li, Z., Zhang, C., Chen, F., Lin, J., Cui, D. and Chen, X., "Chiral guanosine 5'-monophosphate-capped gold nanoflowers: Controllable synthesis, characterization, surface-enhanced Raman scattering activity, cellular imaging and photothermal therapy," *Nano Research* 5(5), 630-639 (2012).
- [49] Qin, L., Huang, D., Xu, P., Zeng, G., Lai, C., Fu, Y., Yi, H., Li, B., Zhang, C. and Cheng, M., "In-situ deposition of gold nanoparticles onto polydopamine-decorated g-C<sub>3</sub>N<sub>4</sub> for highly efficient reduction of nitroaromatics in environmental water purification," *J. Colloid. Interf. Sci.* 534(24), 357-369 (2019).
- [50] Gupta, V. K., Atar, N., Yola, M. L., Üstündağ, Z. and Uzun, L., "A novel magnetic Fe@ Au core-shell nanoparticles anchored graphene oxide recyclable nanocatalyst for the reduction of nitrophenol compounds," *Water Res.* 48(20), 210-217 (2014).
- [51] Hess, K. L., Medintz, I. L. and Jewell, C. M., "Designing inorganic nanomaterials for vaccines and immunotherapies," *Nano Today* 27(3), 73-98 (2019).



- [52] Jv, Y., Li, B. and Cao, R., "Positively-charged gold nanoparticles as peroxidase mimic and their application in hydrogen peroxide and glucose detection," *Chem. Commun.* 46(42), 8017-8019 (2010).
- [53] Mostafavi, E., Medina-Cruz, D., Kalantari, K., Taymoori, A., Soltantabar, P. and Webster, T. J., "Electroconductive nanobiomaterials for tissue engineering and regenerative medicine," *Bioelectricity* 2(2), 120-149 (2020).
- [54] Zhen, S. J., Fu, W. L., Chen, B. B., Zhan, L., Zou, H. Y., Gao, M. X. and Huang, C. Z., "Vertically aligned gold nanomushrooms on graphene oxide sheets as multifunctional nanocomposites with enhanced catalytic, photothermal and SERS properties," *RSC Adv.* 6(96), 93645-93648 (2016).
- [55] Eisen, C., Chin, J. M. and Reithofer, M. R., "Catalytically Active Gold Nanomaterials Stabilized by N-heterocyclic Carbenes," *Chem. Asian J.* 16(20), 3026-3037 (2021).
- [56] Gao, L. and He, C., "Application of nanomaterials decorated with cyclodextrins as sensing elements for environment analysis," *Environ. Sci. Pollut.* 28(42), 59499-59518 (2021).
- [57] Seo, Y. S., Ahn, E.-Y., Park, J., Kim, T. Y., Hong, J. E., Kim, K., Park, Y. and Park, Y., "Catalytic reduction of 4-nitrophenol with gold nanoparticles synthesized by caffeic acid," *Nanoscale Res. Lett.* 12(7), 1-11 (2017).
- [58] Li, L. and Weng, J., "Enzymatic synthesis of gold nanoflowers with trypsin," *Adv. Funct. Mater.* 21(30), 305603 (2010).
- [59] Niazi, S., Khan, I. M., Akhtar, W., Ul Haq, F., Pasha, I., Khan, M. K. I., Mohsin, A., Ahmad, S., Zhang, Y. and Wang, Z., "Aptamer functionalized gold nanoclusters as an emerging nanoprobe in biosensing, diagnostic, catalysis and bioimaging," *Talanta* 268(8), 125270 (2023).
- [60] Fan, K., Wang, H., Xi, J., Liu, Q., Meng, X., Duan, D., Gao, L. and Yan, X., "Optimization of Fe<sub>3</sub>O<sub>4</sub> nanozyme activity via single amino acid modification mimicking an enzyme active site," *Chem. Commun.* 53(2), 424-427 (2017).
- [61] Meng, X., Zare, I., Yan, X. and Fan, K., "Protein-protected metal nanoclusters: An emerging ultra-small nanozyme," *Wires. Nanomed. Nanobi.* 12(3), e1602 (2020).
- [62] Yagati, A. K., Lee, T., Min, J. and Choi, J.-W., "Electrochemical performance of gold nanoparticle–cytochrome c hybrid interface for H<sub>2</sub>O<sub>2</sub> detection," *Colloid. Surface. B.* 92(9), 161-167 (2012).
- [63] Choi, Y., Choi, M.-J., Cha, S.-H., Kim, Y. S., Cho, S. and Park, Y., "Catechin-capped gold nanoparticles: green synthesis, characterization, and catalytic activity toward 4-nitrophenol reduction," *Nanoscale Res. Lett.* 9(103), 1-8 (2014).